BCSIR

Available online at www.banglajol.info

Bangladesh J. Sci. Ind. Res. **58(1)**, 53-64, 2023

BANGLADESH JOURNAL OF SCIENTIFIC AND INDUSTRIAL RESEARCH

E-mail: bjsir07@gmail.com

Electronic, structural and optical properties of Gd-doped ZnO powder synthesized by solid-state reaction method

M. K. Gora[1]*, A. Kumar[1], B. L. Choudhary[2], S. N. Dolia[1], S. Kumar[1] and R. K. Singhal[1]

[1]*Department of Physics, University of Rajasthan, Jaipur-302004, Rajasthan, India*

[2]*Department of Physics, BansathaliVidhyapith, Banasthali-304022, Rajasthan, India*

Abstract

We explored the impact of Gd doping on the structural, electronic and optical characteristics of the ZnO powder. The Gd-doped ZnO (0, 2% and 5%) powder samples have been synthesized using the conventional solid-state reaction process with varied Gd concentrations. The XRD pattern confirmed that all the studied samples are in the hexagonal wurtzite crystalline structure. The morphology has been explored using SEM images, which exhibited an agglomerated rod-like particle structure. The XPS results indicate the presence of oxygen vacancies (V_o) in the Gd-doped ZnO samples and the V_o's are found to increase with increasing Gd amount. According to PL findings, the intensity ratio of the green and ultra-violet emission peaks is found to increase from 0.090 to 0.418 with increasing Gd-doping concentrations, confirming that V_o's are increasing with Gd-doping. The UV-visible spectroscopy results reveal that the energy band gap (E_g) decreased from 3.31 eV to 3.23 eV with increasing Gd-doping concentration.

Received: 23 November 2022

Revised: 05 January 2023

Accepted: 15 January 2023

DOI: https://doi.org/10.3329/bjsir.v58i1.63634

Keywords: Polycrystalline; Rietveld refinement; Wurtzite structure; Oxygen vacancies; XPS; PL

Introduction

Diluted magnetic semiconductor materials are used in optoelectronic and magneto-electronic devices that involve electron charge and spin (Thangeeswari *et al.* 2015). When a traditional semiconductor like ZnO is doped with transition metal (TM) ions or rare-earth (RE) metals, the DMS material could realize. Numerous applications in the spintronics of zinc oxide have piqued the curiosity of researchers. The wide band gap energy of the ZnO is 3.37 eV and the exciton binding energy is 60 m eV, making it perfect for use in light-emitting diodes (Shimogaki *et al.* 2015; Thangeeswari *et al.* 2015). The magnetic, optical, and electrical characteristics of ZnO could be modified by the doping of TM ions and RE elements, which depend on the dopants' nature, quantity, and synthesis process (Deshmukh *et al.* 2010). In particular, ZnO is receiving much attention as a potential material for UV and visible light emitters (Ozgür *et al.* 2005; Fan *et al.* 2013). The visible emission of ZnO is because of several bands associated with various lattice flaws. Consequently, defect-related emission in ZnO displays a wide unstructured band spanning the blue to red spectral regions. Because of this uniqueness, ZnO is a promising phosphor for white-light emitters with a high colour rendering index (Fan *et al.* 2013). ZnO has unique characteristics like affordability, long-term stability, an environmentally friendly nature, better radiation resistance, etc. Additionally, ZnO is an excellent material for several photonic applications when doped with a suitable dopant (Bahadur *et al.* 2007). Doping is a valuable method for modifying the optical characteristics of ZnO due to its ability to exhibit many absorption transitions in the visible region.

*Corresponding author e-mail: gora.phy@gmail.com

RE elements, such as Gd, may introduce additional capabilities to the ZnO system because they may be capable of constructing combined practical devices on a single chip by combining magnetic and optical properties (Ohno *et al.* 1996; Tawil *et al.* 2011).

Rare-earth (RE) metal doping in the dilute magnetic semiconductor (DMS) systems has recently received immense attention due to its potential usage in magneto electronic and photonic devices (Monteiro *et al.* 2006). The influence of Gd doping on the optical and electrical properties of ZnO is crucial for developing optoelectronic devices and understanding the genesis of ferromagnetism. Ma and Wang (2012) synthesized the Gd-doped ZnO nanocrystals using the thermal evaporation deposition method. According to their findings, Gd doping has an appreciable impact on the optical characteristics of the ZnO. The strong UV and blue emissions are detected at low Gd concentrations because Gd impurities introduce a mid-gap state into ZnO. In comparison, the UV and blue emissions reduce for high doping concentrations as a significant broad defect emission appears because of the vast numbers of defects, impurities, and excess Gd_2O_3 produced. Gd-doped ZnO nanocrystals can be used in optoelectronic devices. The optical and electrical tuning of the carrier density and optical band gap energy is essential for developing luminescent materials and equipment based on the ZnO DMS systems. The optical band gap and carrier concentration are essential parameters to yield information about the emission wavelength. Several development characteristics, like the synthesis methods, impurity concentration and substrate variety have been reported to influence these parameters (Wakano *et al.* 2001; Tan *et al.* 2011; Murtaza *et al.* 2011).

The synthesis of DMS materials with unique optical, photocatalytic and magnetic characteristics seems to be the most promising candidate for the subsequent generation of electronic, optoelectronic and spintronic appliances (Kumar and Sahare 2014). The low-dimension materials with imperfection-free lattice structures have excellent electrical and magnetic characteristics; purposefully made or accidental structural defects play a significant role in altering their features (Li *et al.* 2016; Obeid *et al.* 2018). Thus, the presence of different kinds of cation or anion vacancies and interstitials in ZnO nanocrystals may change their magnetic properties, photoluminescence, and photocatalytic properties (Coey *et al.* 2005). Although certain experimental and theoretical findings based on DFT indicate that Gd-doped ZnO exhibits the room temperature ferromagnetism (RTFM) (Potzger *et al.* 2006; Aravindh *et al.* 2014) property, several studies have demonstrated that the RTFM is not present (Sambasivam *et al.* 2015). In addition to their magnetic qualities, the *4f* ions doped ZnO nanocrystals also have an attractive optical responsiveness. Many theoretical and experimental studies showed that RE-doped ZnO could reportedly absorb ultraviolet (UV) light (Chakraborty *et al.* 2017). Obeid *et al.* (2019) prepared undoped and Gd-doped ZnO nanocrystalline samples using the thermal decomposition method. They observed that the optical absorption spectra of pristine ZnO increased with a 6% Gd doping concentration and the magnetic properties changed with changing dopant amounts. Their PL spectroscopy results showed the existence of defects, which increased with increasing Gd doping concentrations. They suggested that these DMS nanoparticles can be used for magneto-optoelectronic practical device applications.

Undoubtedly, the RE-doped ZnO nanostructures have been intensively studied recently because this is a rapidly growing field due to their multi-functionality and their use in possible new generation applications. With an aim to understand the effect of Gd doping in ZnO in terms of its electronic and optical properties we have synthesize Gd-doped ZnO powder series of different Gd (0%, 2%, and 5%) values. Various characterization techniques have been utilized to explore the electronic, structural and optical features of the synthesized powder series. Gd doping into ZnO produced changes in the band gap and enhanced oxygen vacancies related states in the compound.

Materials and methods

The Gd-doped ZnO powder samples with varying Gd (0%, 2%, and 5%) concentrations have been synthesized using the conventional solid-state reaction method. A suitable amount of high-purity (99.999% Sigma-Aldrich) zinc oxide (ZnO) and gadolinium oxide (Gd_2O_3) powder have been used for their preparation. For achieving perfect homogeneity, the ingredients were properly pounded for ~8 hours in an agate mortar and pestle. The prepared material has been sintered for ~8h at~550°C and cooled at room temperature. Again, the mixture was ground for ~2 hours and sintered for ~6 hours at ~550°C. The mixture was milled for ~4 hours before being turned into pellets. Finally, these pellets were sintered for around ~8 hours at about ~600°C. Finally, we ground the pellets to make the powder. The powder form of the prepared samples has been used for further characterization.

Characterization techniques

The crystallographic structures of the samples have been explored using an X-ray diffractometer (Make: Panalytical X'Pert PRO) using the photon energy of Cu Kα (λ= 1.5406Å). SEM images have been used for the morphology study of the synthesized samples. The SEM equipment model

ETH 30 kV EVO-18 Carl Zeiss, with a tilt of 0° to 60° and a rotation of 360°, has been used for taking SEM images.The defect-related states and chemical analysis of the samples have been determined using X-ray photoelectron spectroscopy. A hemispherical analyzer with a 128-channel detector and a monochromated, fully integrated K-alpha small-spot X-ray photoelectron spectrometer system of 180° double focusing is used in XPS (Thermo Scientific made). The UV-visible absorption spectroscopy (Model: Shimadzu UV-3600 UV-VIS-NIR Spectrophotometer) was used to explore the prepared samples' optical absorption and band gap. The measurements of UV-visible absorption spectra have been taken using the powder form of the samples. PL spectroscopy was used to analyze defect-related states in the prepared samples. Photoluminescence spectra have been recorded at room temperature using the fluorescence spectrometer (Model: Perkin Elmer FL 8500).

Results and discussion

XRD analysis

Fig. 1. depicts the powder XRD patterns of the Gd-doped ZnO (Gd = 0%, 2%, and 5%) samples. All the diffraction peaks detected in the ZnO sample match with the standard JCPDS card number (36-1451). This confirms a hexagonal wurtzite crystal structure of the samples.

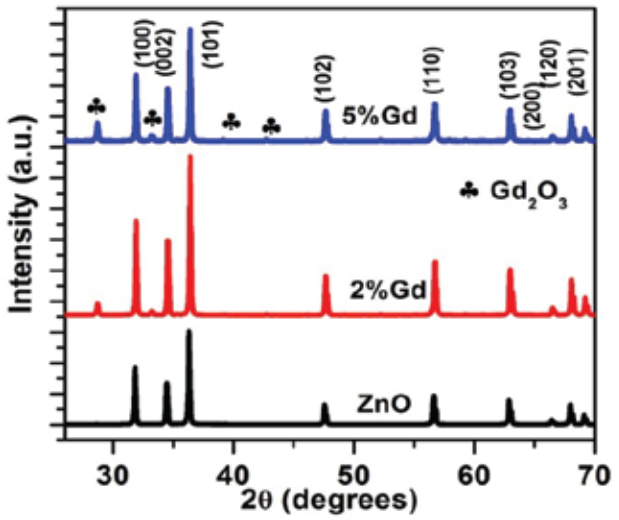

Fig. 1. XRD patterns for the pure ZnO powder (Gora *et al.* 2022) and (2% and 5%) Gd-doped ZnO powder samples

The diffraction peaks were observed at 31.88°, 34.50°, 36.25°, 47.72°, 56.69°, 63.03°, 66.59°, 68.17°, and 69.35°, which are related to the planes (100), (002), (101), (102), (110), (103), (200), (112), and (201), respectively (Ganesh *et al.* 2018; Bharathi *et al.* 2020). Further, some additional small peaks have been observed at 28.61°, 33.21°, and 39.14° with increasing Gd doping. These secondary peaks representing a crystallite phase have been identified as Gd_2O_3, which is well consistent with earlier reports (Das *et al.* 2012). As shown in Fig. 2, the highest intense peak related to the (101) plane shifted slightly higher angles with the increasing concentration of Gd doping. The shift is because of the substitution of bigger-sized Gd^{3+} (0.94 Å) ions than Zn^{2+} (0.74 Å) ions in the hexagonal wurtzite structure. The peak shift may indicate that Gd^{3+} ions have occupied the crystallographic positions of Zn^{2+} ions in the ZnO host lattice, or itmay be because of the structural strain caused by the formation of internal compressive micro stress (Dakhel and El-Hilo 2010; Kumar *et al.* 2014; Sahu *et al.* 2017).

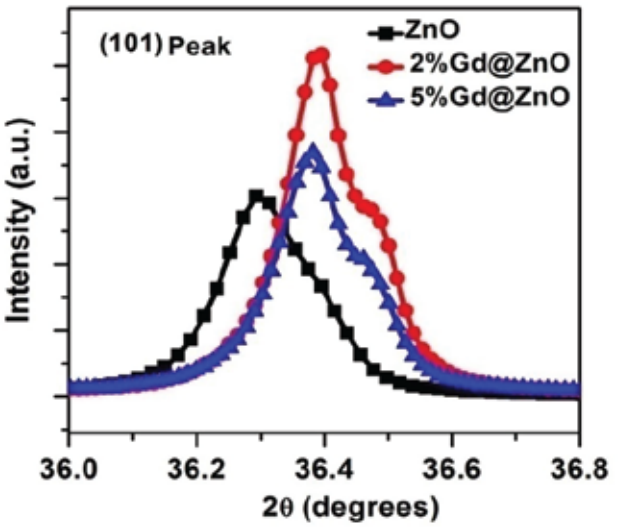

Fig. 2. Extended XRD patterns for the (101) peak of undoped ZnO powder (Gora *et al.* 2022) and Gd-doped ZnO (Gd = 2% and 5%) powder samples

Rietveld refinements have been performed using the Full Prof Programme (shown in Fig. 3). The Pseudo-Voigt function has been used for Rietveld refinement of all the samples with the space group $P6_3mc$. The estimated lattice parameters have been listed in Table I. The lattice parameters are found to decrease with Gd doping, similar to those reported in earlier studies (Kaur *et al.* 2016; Obeid *et al.* 2019). The factors like the induced deficiencies (vacancies, interstitial) and the ionic radius of Zn and Gd ions can be responsible for the observed change (Kaur *et al.* 2016; Kumar and Thangavel 2017).

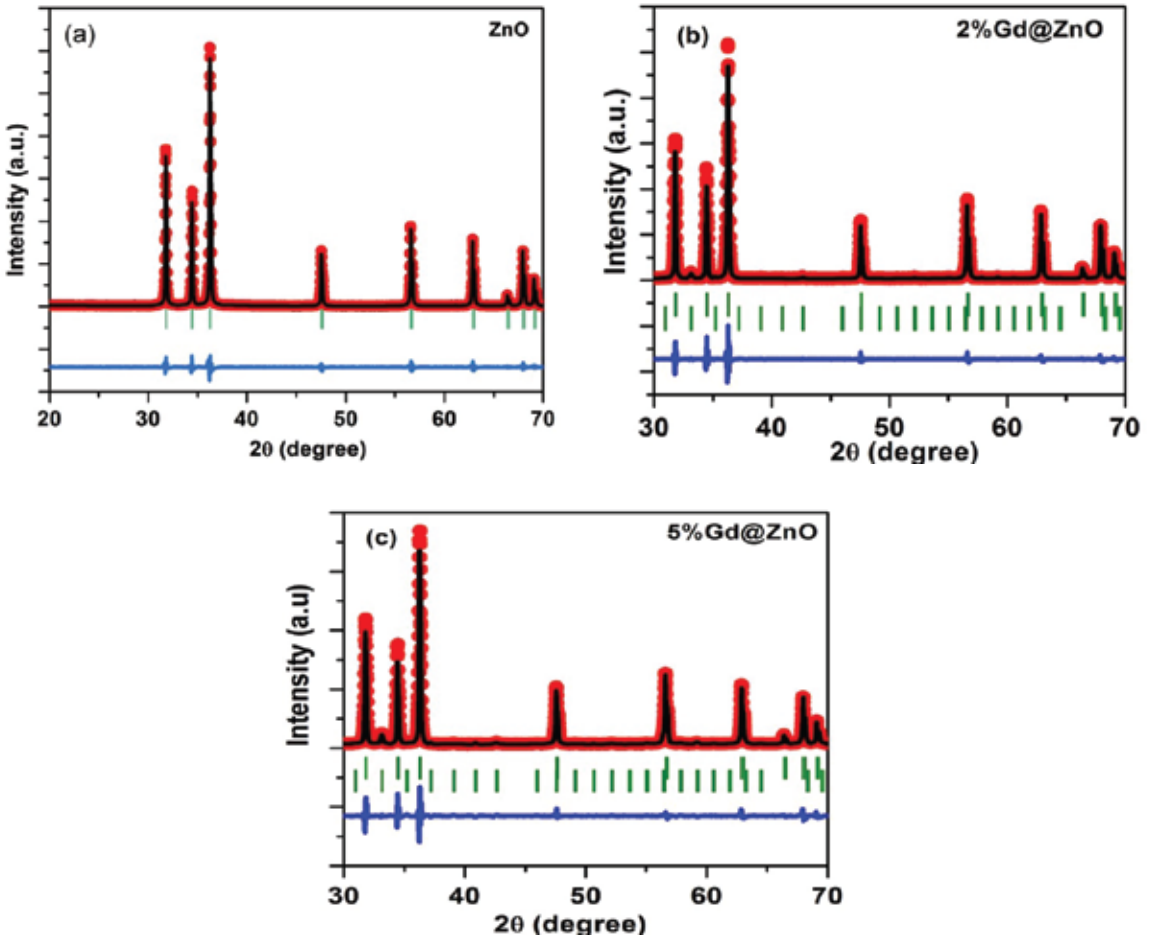

Fig. 3. Rietveld refined XRD patterns for polycrystalline powder samples of (a) the pure ZnO (Gora *et al.* 2022), (b) the 2% Gd-doped ZnO and (c) the 5% Gd-doped ZnO. Observed data is shown by red dots and black solid line is the fitted profile. Bragg peak positions are marked by vertical green lines. The lower plot in blue is the residual curve

Table I. Lattice parameters and c/a ratio of the Gd-doped ZnO polycrystalline powder samples

Sample	Lattice Parameter Å		c/a
	a	c	
ZnO	3.2505	5.2077	1.6
2% Gd@ZnO	3.2498	5.2059	1.6
5% Gd@ZnO	3.2490	5.2047	1.6

SEM analysis

Scanning electron micrographs have been used to analyze the morphology of the Gd-doped ZnO powder samples. The SEM images reveal a rod-like morphology in pure ZnO (Gora *et al.* 2022) and the Gd-doped ZnO polycrystalline samples with some proof of agglomeration and phase segregation, as depicted in Fig. 4 (a, b and c). Profound observation of the particles exhibits that the crystallite size is above 100 nm. The particles were intensive and incompatibly distributed all over the mass. A distinct boundary between neighbouring crystallites can be noticed, despite the proximity of these smaller crystallites.

XPS analysis

The XPS technique is an excellent tool for determining the surface chemistry and electron configuration of the various elements present in a multicomponent material. The carbon C*1s* peak (284.6 eV) has been used as a refer-

ence to calibrate all the binding energies of the spectra. The survey spectrum of the Gd-doped ZnO samples is shown in Fig. 5. The survey spectra revealed the existence of O, Zn, and Gd elements without any impurity in the samples.

For ZnO and 2% Gd-doped ZnO powder samples, the binding energies of the Zn$2p_{3/2}$ and Zn$2p_{1/2}$ peaks are found to be 1021.25 eV, 1044.25 eV, 1021.43 eV, and 1044.43 eV, respectively. However, for the 5% Gd-doped ZnO sample, these peaks are at 1021.83 and 1044.83 eV energy positions. The small shift could be assigned to the creation of Zn interstitials in ZnO upon Gd doping. The binding energy gap between the zinc doublet peaks has been found at about 23 eV. This indicates that Zn in the ZnO crystal structure is in the Zn^{2+} oxidation state (Khataee *et al.* 2015; Gawai *et al.* 2019) as the spin-orbital splitting of Zn*2p* is 23 eV. This difference does not change with the Gd doping pointing out that Gd doping has no discernible effect on the chemical position of ZnO.

The O*1s* asymmetric XPS spectraare shown in Fig.7 (a) which is asymmetric in shape. The O*1s* XPS spectra of all these samples i.e. the ZnO, the $Zn_{0.98}Gd_{0.02}O$, and the $Zn_{0.95}Gd_{0.05}O$ have been deconvoluted mainly into two Gaussian peaks, as shown in Fig. 7 (b, c, and d). The lower binding peaks for pure and Gd-doped ZnO (Gd = 2% and 5%) polycrystalline samples have been detected at 529.93 eV, 529.93 eV and 529.78 eV, respectively, which attributed to the lattice oxygen in the hexagonal structure of the ZnO.

The higher binding peak for the pure and the Gd-doped ZnO samples have been found at 531.51 eV, 531.66 eV, and 531.49 eV, respectively, which is due to the presence of oxygen vacancies in the ZnO structure (Bharathi *et al.* 2020; Sukumaran *et al.* 2021). An additional signal centered at 528.29 eV has been detected in the 5% Gd-doped ZnO powder sample, which could be ascribed to the coordination of oxygen in Gd-O-Zn along grain boundaries because of the excessive Gd dopants and also attributed to the presence of

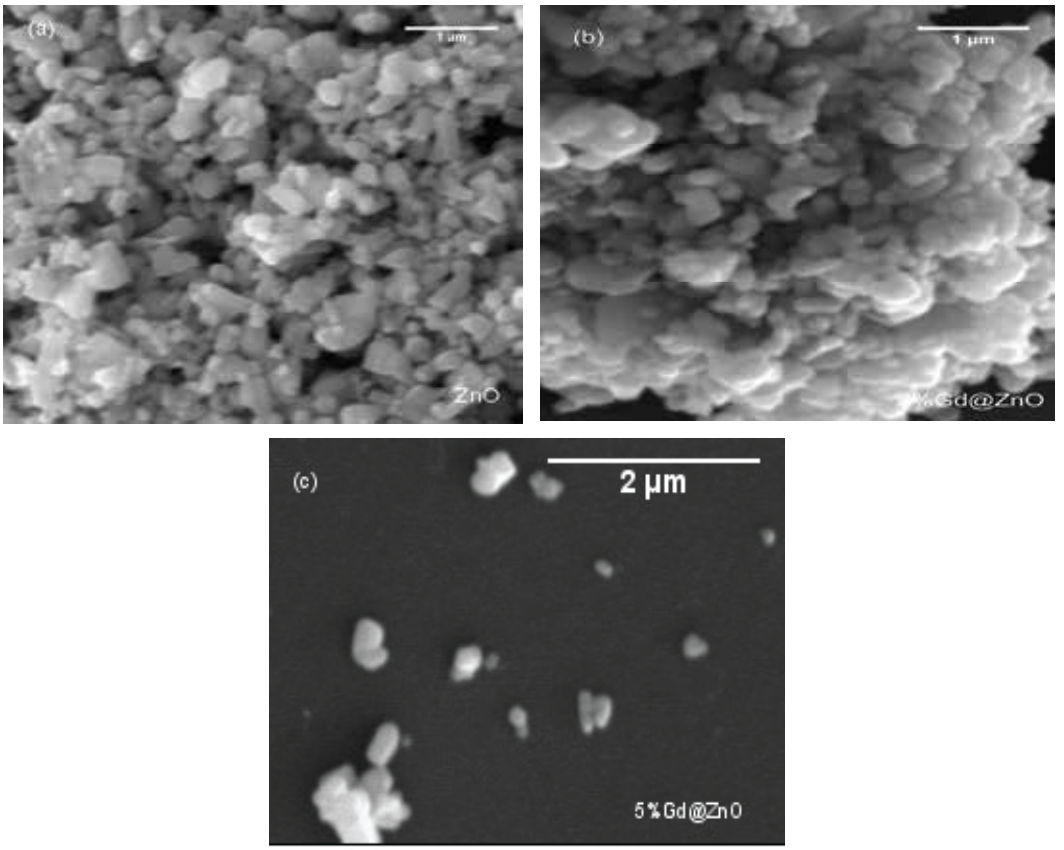

Fig. 4. SEM images of prepared polycrystalline powder samples: (a) for the ZnO (Gora *et al.* 2022), (b) for the 2% Gd-doped ZnO and (c) for the 5% Gd- doped ZnO

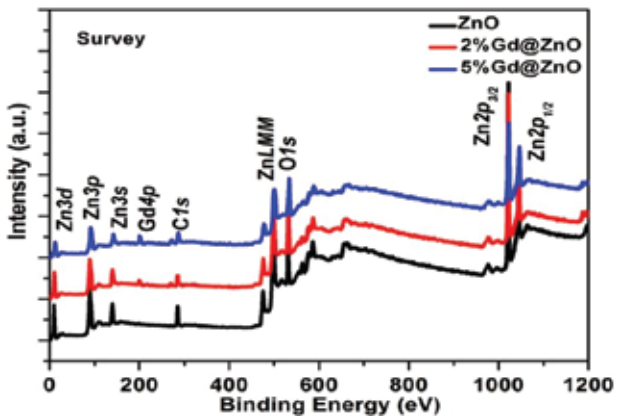

Fig. 5. The XPS survey spectra of the pure ZnO (Gora *et al.* 2022), the $Zn_{0.98}Gd_{0.02}O$ and the $Zn_{0.95}Gd_{0.05}O$ powder samples

The Zn*2p* core level spectra of the Gd-doped ZnO samples are depicted in Fig. 6.

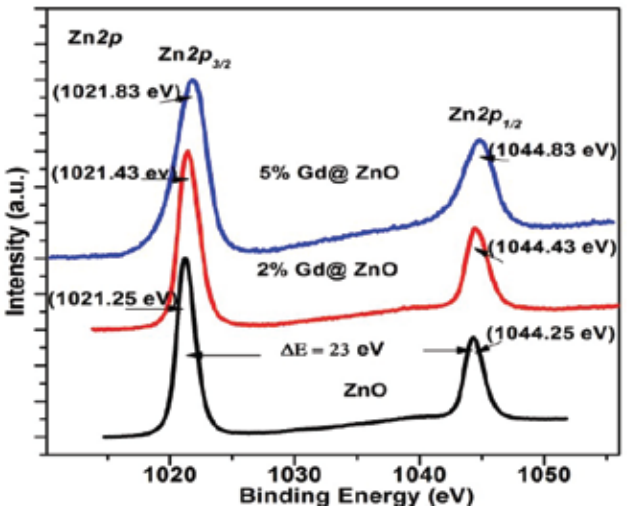

Fig. 6. The Zn2p core level XPS spectra of the Gd-doped ZnO polycrystalline powder samples

Gd_2O_3 in the sample (Yi *et al.* 2017). The lattice oxygen peak has slightly shifted to the lower binding energy with increasing Gd concentration, which has been due to the increased oxygen vacancies with increasing Gd doping. The estimated area ratios of the oxygen vacancies peak and the lattice oxygen peak for the samples ZnO, $Zn_{0.98}Gd_{0.02}O$, and $Zn_{0.95}Gd_{0.05}O$ comes out to be 0.53, 1.30, and 2.49, respectively. These results show that the oxygen vacancies increase with increasing Gd concentration.

The Fig. 8 (a, b) depicts the high-resolution Gd*4d* XPS spectra of the Gd-doped samples.In the Gd*4d* state, the spin-orbit splatted peaks are at 144.6 eV for $Gd4d_{3/2}$ and 139.6 eV for $Gd4d_{5/2}$ for the 2% Gd-doped sample, whereas for the 5% Gd-doped ZnO sample, the spin-orbit splits at 145.5 eV for $Gd4d_{3/2}$ and 139.7 eV for $Gd4d_{5/2}$ as shown in Fig. 8 (a, b). This indicates that Gd is present in the Gd^{3+} state in the ZnO hexagonal structure. The shift in peak values of $Gd4d_{3/2}$ and $Gd4d_{5/2}$ from 144.6 eV and 139.6 eV, respectively; in the case of 2% Gd-doped sample to 145.5 eV and 139.7 eV, respectively, in the case of 5% Gd-doped sample. This shift in Gd*4d* peaks is ascribed to the electron transfer from plasmonics Gd to ZnO because of the strong electronic interaction (covalent bond) between Gd and the oxide (Ahmad *et al.* 2011; Wang *et al.* 2012; Bharathi *et al.* 2020).

UV visible spectroscopy analysis

The UV–Visible spectroscopy is a powerful tool for estimating band gap of materials. UV–Vis absorbance spectra and tauc plots for the Gd-doped ZnO samples (Gd = 0% (Gora *et al.* 2022), 2%, and 5%) samples are shown in Figs.9 (a, b, c, and d). The spectra show a red shift with increasing Gd amount in the ZnO.The UV–Vis absorption intensity of the synthesized polycrystalline samples is found to reduce with the increasing Gd concentration (Mazhdi and Tafreshi 2018). Tauc's plot has been used to calculate the direct band gap of the samples (Jain *et al.* 2006). The direct band gap has been estimated using the following equation:

$$\alpha h\upsilon = A\,(h\upsilon - E_g)^{1/2}$$

Here, α is the absorption coefficient,υ is frequency, h is the Planck constant, A is a constant, and E_g is the energy band gap of the substance.

Extrapolating the linear component of the curve plotted among $(\alpha h\upsilon)^2$ and hυ depicted in Fig. 9 (b, c, and d) has been used to obtain the band gap (Farhad *et al.* 2018; Ghos *et al.* 2021). The band gap values calculated for the Gd-doped ZnO samples, i.e.are 3.31 eV (Gora *et al.* 2022), 3.27 eV, and 3.23eV, for the samples Gd = 0%, 2% and 5%, respectively. The small redshift observed in the band gap of Gd-doped ZnO samples is because of the changes in electronic structure as well as enhanced oxygen vacancies with the increasing Gd doping (Yi *et al.* 2017; Flemban *et al.* 2016), which is responsible for the band gap reduction.

Photoluminescence spectroscopy analysis

The structural flaws like ionic and atomic vacancies, replacements and interstitials have been explored using the PL

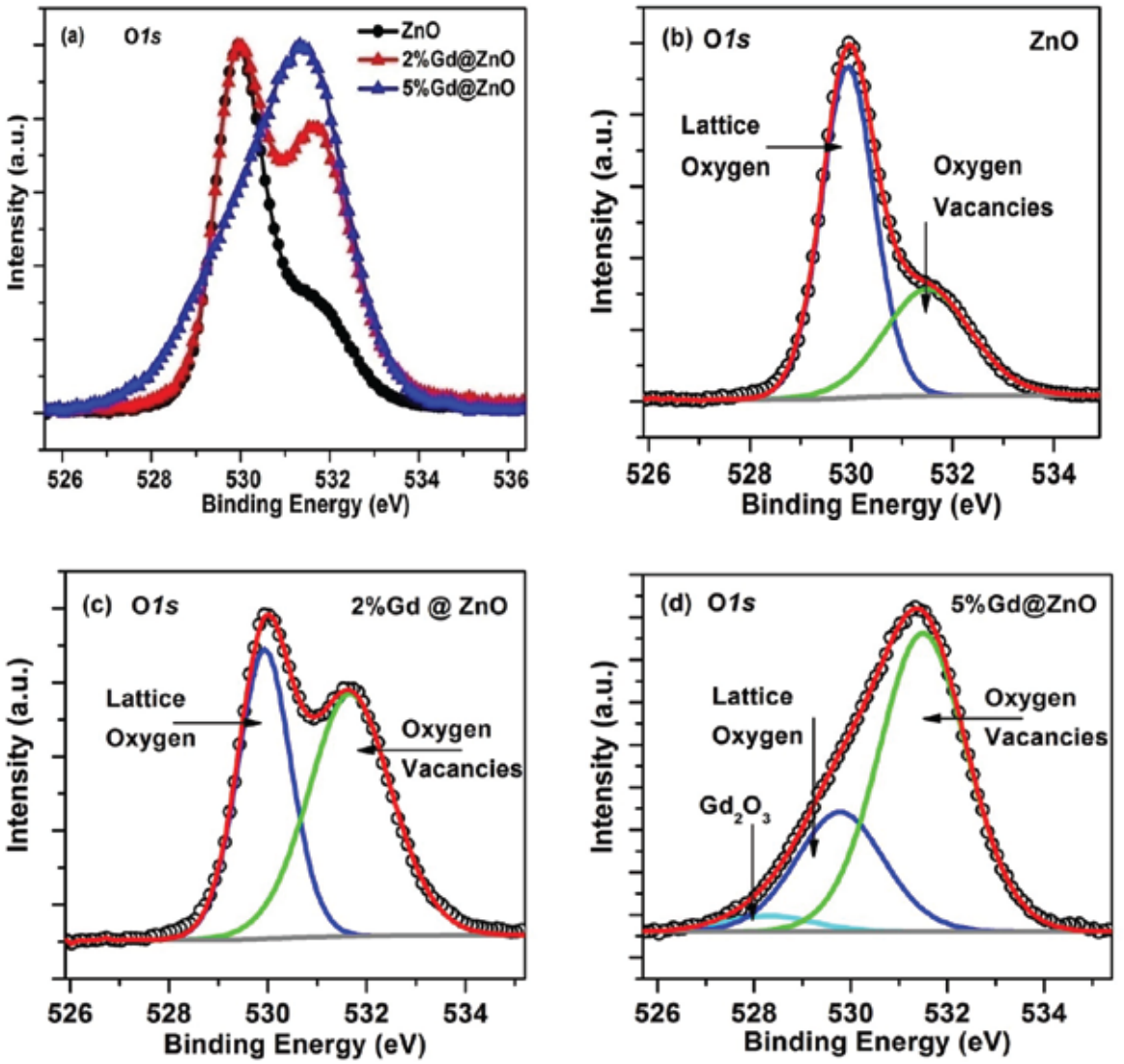

Fig. 7. O1s XPS spectra: (a) asymmetric spectra for all Gd-doped ZnO bulk samples (Gd = 0%, 2% and 5%); (b) for the ZnO: fitted with two Gaussian peaks; (c) for the 2% Gd-doped ZnO polycrystalline sample: fitted with two Gaussian peaks; (d) for the 5% Gd-doped ZnO polycrystalline powder sample: fitted with three Gaussian peaks

spectra of the synthesized polycrystalline samples. Fig. 10 (a, b and c) shows the deconvoluted, Gaussian-fitted PL spectra of the synthesized Gd-doped ZnO polycrystalline powder samples.

The PL spectra of the samples were recorded at room temperature in order to determine the types of vacancies, defect band emission etc. (Lin *et al.* 2001; Yi *et al.* 2017). The photoluminescence spectra have been deconvoluted and the different peaks responsible for the emission have been Gaussian fitted. For these samples the band edge emission peaksare detected at 381 nm, 384 nm, and 383 nm, for the Gd = 0%, 2% and 5% samples, respectively. The UV emission is responsible for the excitonic interaction related to the band edge emission. The intense violet emission exhibited in the Gd-doped ZnO at about 415 nm could be because ofthe oxygen vacancies. The exciton interaction between the holes in the valence band and electrons located in the interstitial zinc could be responsible for the violet emission peak at about 447 nm. Intrinsic deficiencies like interstitial zinc and

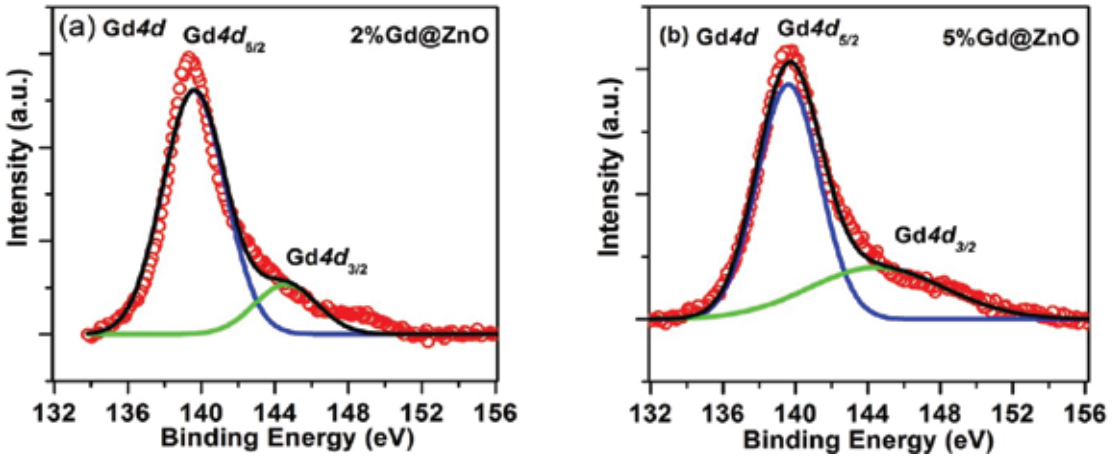

Fig. 8. The Gd4dXPS spectra for (a) 2% Gd-doped ZnO bulk sample and (b) 5% Gd-doped ZnO bulk sample

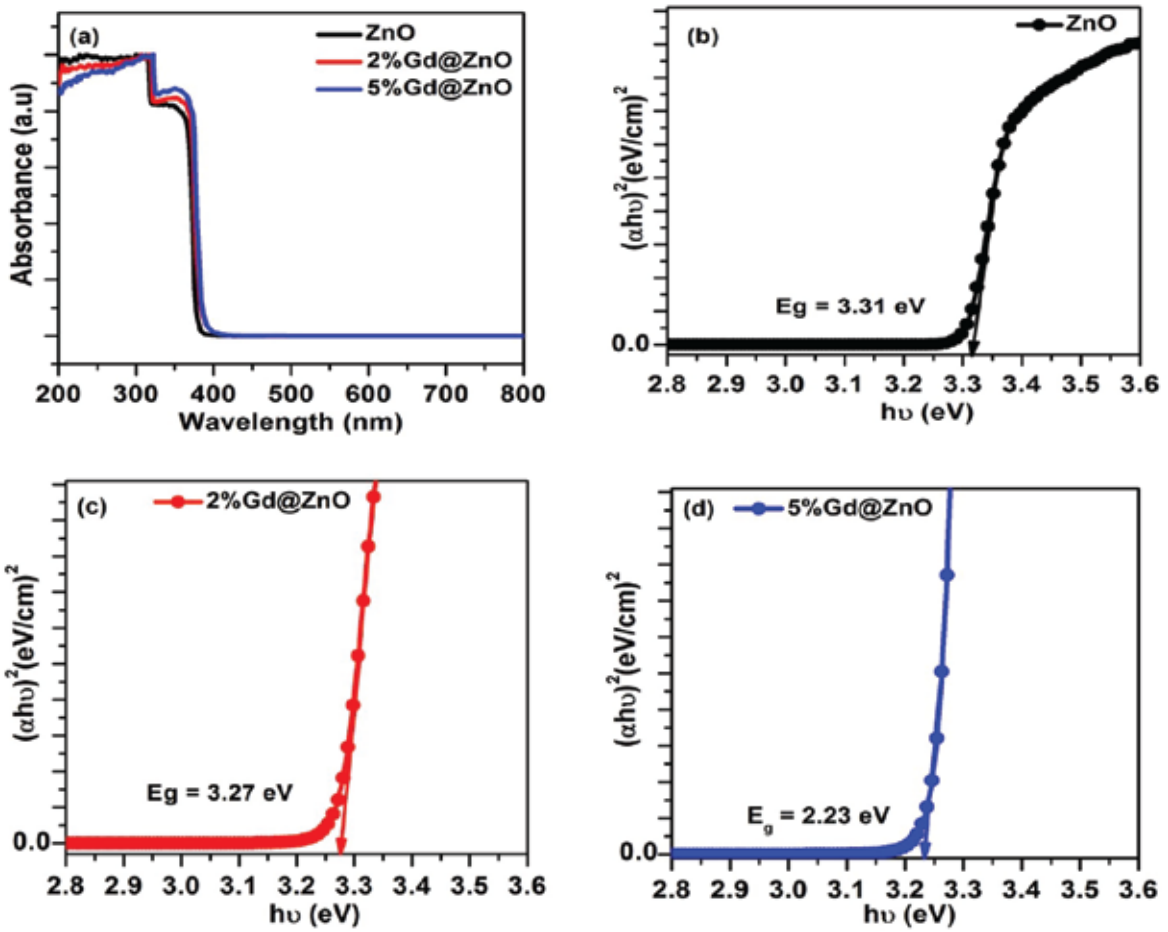

Fig. 9. (a) UV–visible spectra of Gd-doped ZnO (pure ZnO (Gora *et al.* 2022); Gd = 2% and 5%) and Tauc plots of the synthesized powder samples: (b) for the ZnO (Gora *et al.* 2022), (c) for the 2% Gd-doped ZnO and (d) for the 5% Gd-doped ZnO

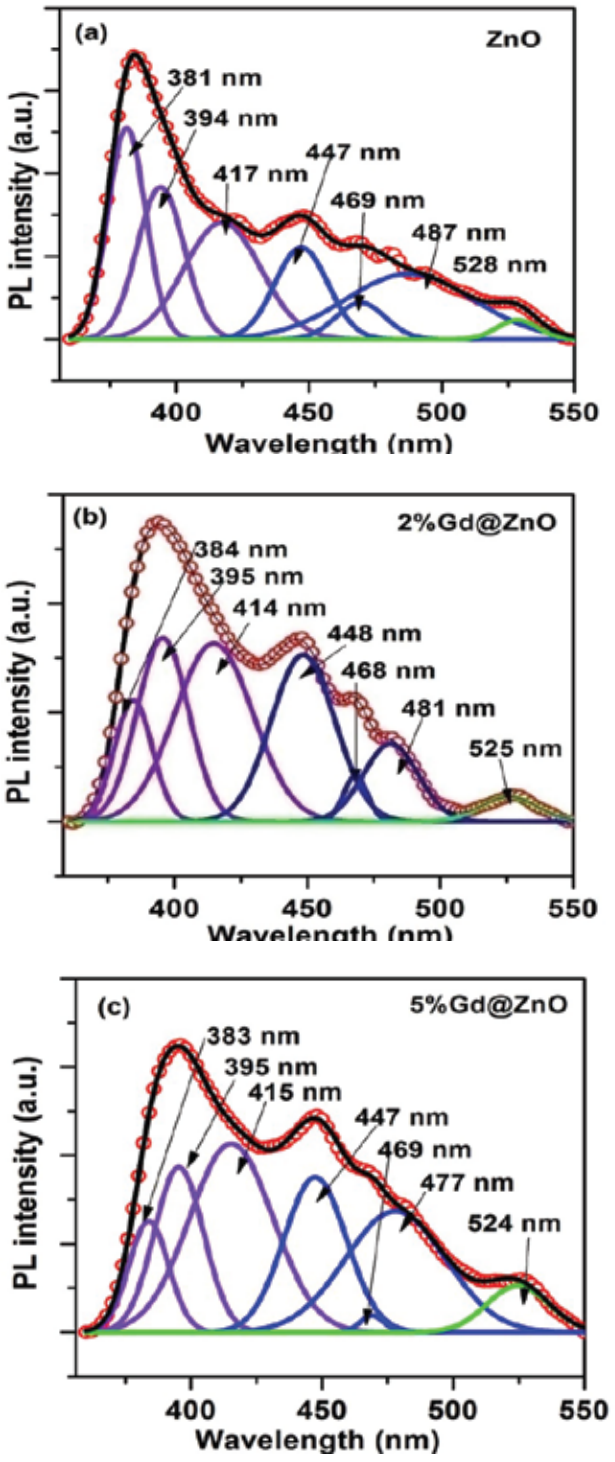

Fig. 10. PL spectra: (a) for ZnO (Gora *et al.*, 2022), (b) for 2% Gd-doped ZnO (c) for 5% Gd-doped ZnO powder sample

oxygen can be attributed to the peak at 477 nm (Singh *et al.* 2009; Kaur *et al.* 2016). The transformation between singly ionized oxygen deficiency and the photo-created holes (Kennedy *et al.* 2014) or the surface imperfection and electrons near the conduction band, might be responsible for the green emission peak seen for the Gd-doped ZnOat around 525 nm. The green emissions are commonly attributed to theoxygen vacancies (Studenikin *et al.* 1998). For Gd-doped ZnO polycrystalline powder samples, the intensity ratio of the green and ultra-violet emission peaks is found to be 0.090 for ZnO, 0.204 for the 2% Gd-doped ZnO, and 0.418 for the 5% Gd-doped ZnO. The defect-related emissions enhanced with increasing Gd doping in the ZnO indicate that a large number of deficiencies, such as oxygen vacancies, are most usually related to crystal deformation (Yi *et al.* 2017). The results reveal that the Gd doping enhances the Zn_i and V_o flaws. It could be attributed to structural deformation created by Gd atoms with different ionic sizes than Zn in the ZnO (Bandopadhyay and Mitra 2015; Sukumaran *et al.* 2021). Increasing Gd doping in ZnO indicates an increase in defect states, which matches well with the XPS results.

We compared our PL results with Farhad *et al.* (2019), who prepared ZnO DC (drop casting) and ZnO nanorods. Their PL results detected the PL peak at 380 nm and a barely observable green-yellow emission peak; in our case, we find it at 381 nm for ZnO, 384 nm for 2% Gd-doped ZnO and 383 nm for the 5% Gd-doped ZnO polycrystalline sample. This peak represented ZnO's near band edge (NBE) transition because of free excitons recombinations and this PL property indicates high crystalline quality. The luminescent characteristics in the visible region are responsible for the different defects, like zinc interstitials (Zn_i), oxygen vacancies (V_o), etc., present in the ZnO crystal matrix. As a result, they reported that both ZnO (DC) and ZnO nanorods were found to be defect-free good crystalline and optical properties materials. In our case, all the prepared Gd-doped ZnO powder samples have been found to be with single ionized oxygen vacancies, which are confirmed by the green emission peak at 525 nm in the PL spectra.

Conclusion

The Gd-doped ZnO powder samples were synthesized by the solid-state reaction method. The XRD patterns affirm that Gd has been successfully incorporated into the ZnO lattice and confirm the hexagonal wurtzite structure. SEM images have been used to reveal the morphologies of the synthesized samples, which appear as rod-like structures. The XPS results showed that the oxygen vacancy-related states in Gd-doped samples increased with increasing Gd doping. PL findings confirmed that the defect-related states are present

in the Gd-doped ZnO polycrystalline samples. The green emission and ultra-violet emission peaks' intensity ratio is 0.418 for the 5% Gd-doped ZnO sample, which is the maximum compared to the pure ZnO and 2% Gd-doped ZnO polycrystalline powder sample. These findings confirmed that the oxygen vacancies increase as the Gd concentration increases and the PL results agree well with the XPS results. The UV absorption spectra findings reveal that the band gap in the 5% Gd-doped ZnO sample is found to be 3.23 eV, which is the minimum compared to both the pure ZnO and the 2% Gd-doped ZnO samples, confirming that Eg is reduced with increasing Gd concentration.

Acknowledgment

The authors are thankful to USIC, University of Rajasthan, Jaipur, Rajasthan (India), for providing SEM images of the prepared samples. We also thank department of physics, BanasthaliVidhyapith, Banasthali, Jaipur, Rajasthan (India) for rendering XRD data.

Funding sources

This research is not financed by any agency.

Authors' contribution

Sample preparation, data analysis, manuscript composition and writing (Mahendra Kumar Gora); sample synthesis and data characterization (Arvind Kumar); data recording (Banwari Lal Choudhary); data analysis and interpretation (Sanjay Kumar); reviewing and editing (Satya NarainDolia); supervision, writing, reviewing and editing (Rishi Kumar Singhal).

Conflicts of interest or competing interests

All authors declare that we have no conflict of interest or competing interests.

Data availability

On request, data will be available.

Ethical approval

Not applicable.

References

Ahmad M, Yingying S, Nisar A, Sun H, Shen W, Wei M and Zhu J (2011), Synthesis of hierarchical flower-like ZnO nanostructures and their functionalization by Au nanoparticles for improved photocatalytic and high performance Li-ion battery anodes, *J. Mater. Chem.* **21:** 7723-7729. https://doi.org/10.1039/C1JM10720H

Aravindh SA, Schwingenschloegl U and Roqan IS (2014), Ferromagnetism in Gd doped ZnO nanowires: a first principles study, *J. Appl. Phys.* **116:** 233-906. https://-doi.org/10.1063/1.4904860

Bahadur H, Srivastava AK, Divi H, Chander H, Basu A, Samanta SB, Sood KN, Kishore R, Sharma RK, Bhatt V, Pal P and Chandra S (2007), Nano-structured ZnO films by sol-gel process, *Indian Journal of Pure and Applied Physics.* **45:** 395-399

Bandopadhyay K and Mitra J (2015), Zn interstitials and O vacancies responsible for n-type ZnO: what do the emission spectra reveal?, *RSC Adv*. **5:** 23540-23547. https://-doi.org/10.1039/C5RA00355E

Bharathi P, Mohan MK, Shalini V, Harish S, Navaneethan M, Archana J, Kumar MG, Dhivya P, Ponnusamy S, Shimomura M and Hayakawa Y (2020), Growth and influence of Gd doping on ZnO nanostructures for enhanced optical, structural properties and gas sensing applications, *Applied Surface Science.* **499:** 143857. https://doi.org/10.1016/j.apsusc.2019.143857

Chakraborty A, Jong CS, Ganguli N and Dasgupta I (2017), A comparative study of magnetic and optical properties of Mn-, Gd-, and Nd-doped ZnO nanowires, *Int. J. Mod. Phys. B*. **31:** 165-241. https://doi.org/10.1142/S0217979216502416

Coey JMD, Venkatesan M and Fitzgerald C (2005), Donor impurity band exchange in dilute ferromagnetic oxides, *Nat. Mater.* **4:** 173-179. https://-doi.org/10.1038/nmat1310

Dakhel AA and El-Hilo M (2010), Ferromagnetic nanocrystallineGd-doped ZnO powder synthesizedby coprecipitation, *Journal of Applied Physics.* **107**: 123-905. doi: 10.1063/1.3448026

Das J, Mishra DK, Sahu DR and Roul BK (2012), Structural and magnetic property of Mn: ZnO bulk ceramic doped with rare earth (Gd/Sm) atoms, *Physica B: Condensed Matter*. **407:** 3575-3579. https://doi.org/10.1016/j. physb. 2012.05.028

Deshmukh AV, Patil SI, Yusuf SM, Rajarajan AK and Lalla NP (2010), Structural, chemical and magnetic investigations of polycrystalline $Zn_{1-x}Mn_xO$, *Journal of Magnetism and Magnetic Materials.* **322:** 536-541. https://doi.org/10.1016/j.jmmm.2009.10.011

Fan JC, Chang SL and Xie Z (2013), ZnO-based light-emitting diodes, *Optoelectronic-Advanced Materials and Devices.* (Ch. 2) doi: 10.5772/51181

Farhad SFU, Tanvir NI, Bashar MS and Sultana M (2019), Synthesis and Characterization of *c*-Axis Oriented Zinc Oxide Thin Film and Its Use for the Subsequent Hydrothermal Growth of Zinc Oxide Nanorods, *MRS Advances.* DOI: 10.1557/adv.2019.65

Farhad SFU, Tanvir NI, Bashar MS, Hossain MS, Sultana M and Khatun N (2018),Facile synthesis of oriented zinc oxide seed layer for the hydrothermal growth ofzinc oxide nanorods, *Bangladesh J. Sci. Ind. Res.* **53**(4): 233-244. DOI: http://dx.doi.org/10. 3329/bjsir.v53i4. 39186

Flemban TH, Sequeira MC, Zhang Z, Venkatesh S, Alves E, Lorenz K and Roqan IS (2016), Identifying the influence of the intrinsic defects in Gd-doped ZnO thin-films, *J. Appl. Phys.* **119:** 65-301. https://-doi.org/10.1063/1.4941434

Ganesh RS, Navaneethan M, Patil VL, Ponnusamy S, Muthamizhchelvan C, Kawasaki S, Patil PS and Hayakawa Y (2018), Sensitivity enhancement of ammonia gas sensor based on Ag/ZnO flower and nanoellipsoids at low temperature. *Sensors Actuators B: Chemical.* **255:** 672-683. https://doi.org/10.1016/j.snb.2017.08.015

Gawai UP, Patil AR, Sonawane TB, Huse VR and Bodke MR (2019), Influence of Gd Substitution on Different Properties of ZnO Nanoparticles, *IOSRJEN.* **09:** 51-57. https://www.researchgate.net/publication/335456724

Ghos BC, Farhad SFU, Patwary MAM, Majumder S, Hossain MA Tanvir NI, Rahman MA, Tanaka T and QixinGuo Q (2021), Influence of the Substrate, Process Conditions, and Postannealing Temperature on the Properties of ZnO Thin Films Grown by the Successive Ionic Layer Adsorption and Reaction Method, *ACS Omega.* **6:** 2665-2674. https://-doi.org/10.1021/acsomega.0c04837

Gora MK, Kumar A, Kumar S, Maheshwari PK, Patidar D, Dolia SN and Singhal RK (2022), Electronic, optical and magnetic properties of Cu-doped ZnO, a possible system for eco-friendly and energy-efficient spintronic applications, *Environmental Science and Pollution Research.*https://doi.org/10.1007/s11356-022-22767-6

Jain A, Sagar P and Mehra RM (2006), Band gap widening and narrowing in moderately and heavily doped n-ZnO films, *Solid-state Electron.* **50:** 1420-1424. https://-doi.org/10.1016/j.sse.2006.07.001

Kaur P, Kumar S, Chen CL, Hsu YY, Chan TS, Dong CL, Srivastava C, Singh A and Rao SM (2016), Investigations on structural, magnetic and electronic structure of Gd-doped ZnO nanostructures synthesized using sol–gel technique, *Appl. Phys. A*. **122:** 161. http://dx.-doi.org/10.1007%2Fs00339-016-9707-5

Kennedy J, Murmu PP, Manikandan E and Lee SY (2014), Investigation of structural and photoluminescence properties of gas and metal ions doped zinc oxide single crystals, *J. Alloy Comp.* **616:** 614-617. http://dx.-doi.org/10.1016%2Fj.jallcom.2014.07.179

Khataee A, Soltani RDC, Karimi A and Joo SW (2015), Sonocatalytic degradation of a textile dye over Gd-doped ZnO nanoparticles synthesized through sonochemical process,*Ultrasonics Sonochemistry*. **23:** 219-230. https://doi.org/10.1016/j.ultsonch.2014.08.023

Kumar S and Sahare P (2014), Gd^{3+} incorporated ZnO nanoparticles: a versatile material, *Mater. Res. Bull*. **51:** 217-223. https://doi.org/ 10.1016/ j.materres-bull.2013.12.031

Kumar S and Thangavel R (2017), Gd doping effect on structural, electrical and magnetic properties of ZnO thin films synthesized by sol-gel spin coating technique, *Electronic Materials Letters.* **13:** 129-135.-doi:10.1007/s13391-017-6164-z

Kumar S, Asokan K, Singh RK, Chatterjee S, Kanjilal D and Ghosh AK (2014), Investigations on structural and optical properties of ZnO and ZnO: Co nanoparticles under dense electronic excitations, *RSC Adv.* **4:** 62123-62131. https://doi.org/10.1039/C4RA09937K

Li X, Ma L, Wang D, Zeng XC, Wu X and Yang J (2016), Point defects in lines in single crystalline phosphorene: directional migration and tunable band gaps, *Nanoscale*. **8:** 17801-17808. https://doi.org/10.1039/C6NR05414E

Lin BX, Fu ZX and Jia Y (2001), Green luminescent center in undoped zinc oxides films deposited on silicon substrates, *Appl. Phys. Lett.* **79:** 943-945. https://-doi.org/10.1063/1.1394173

Ma X and Wang Z (2012), The optical properties of rare earth Gd doped ZnO nanocrystals, *Materials Science in Semiconductor Processing.* **15:** 227-231. doi:10.1016/j.mssp.2011.05.013

Mazhdi M and Tafreshi MJ (2018), The effect of gadolinium doping on the structural, morphological, optical, and photoluminescence properties of zinc oxide nanoparticles prepared by co-precipitation method, *Applied Physics A.* **124:** 863. https://doi.org/10.1007/ s00339-018-2291-0

Monteiro T, Neves AJ, Carmo MC, Soares MJ, Peres M, Alves E, Rita E and Wahl U (2006), Optical and struc-

tural analysis of bulk ZnO samples undoped and rare earth doped by ion implantation, *Superlattices and Microstructures*. **39:** 202-210. https://doi.org/10.1016/j.spmi.2005.08.043

Murtaza G, Iqbal MA, Xu YB, Will IG and Huang ZC (2011), Study of Sm-doped ZnO samples sintered in a nitrogen atmosphere and deposited on n-Si (1 0 0) by evaporation technique*, J.Magn. Magn. Mater.* **323:** 3239-3245. https://doi. org/10.1016/j.jmmm. 2011.07.021

Obeid MM, Jappor HR, Al- Marzoki K, Al-Hydary IA, Edrees SJ and Shukur MM (2019), Unraveling the effect of Gd doping on the structural, optical, and magnetic properties of ZnO based diluted magnetic semiconductor nanorods, *RSC Adv.* **9:** 33207-33221. doi: 10.1039/c9ra04750f

Obeid MM, Mogulkoc Y, Edress SJ, Ciftci YO, Shukur MM and Al-Marzooqee MMH (2018), Analysis of the structural, electronic, elastic and thermodynamic properties of $CuAl_2X_4$ (X = O, S) spinel structure, *Mater. Res. Bull.* **108:** 255-265. https://doi.org/10.1016/j.materresbull.2018.09.013

Ohno H, Shen A, Matsukura F, Oiwa A, Endo A, Katsumoto S and Iye Y (1996), (Ga, Mn) As: A new diluted magnetic semiconductor based on GaAs, *Applied Physics Letters.* **69:** 363-365. https://doi.org/10.1063/1.118061

Ozgür U, Alivov YI, Liu C, Teke A, Reshchikov MA, Dogan S, Avrutin V, Cho SJ and Morkoc H (2005), A comprehensive review of ZnO materials and devices, *Journal of Applied Physics.* **98:** 41-301. https://doi.org/10.1063/1.1992666

Potzger K, Zhou S, Eichhorn F, Helm M, Skorupa W, Mucklich A and Fassbender J (2006), Ferromagnetic Gd-implanted ZnO single crystals*, J. Appl. Phys.* **99:** 63-906. https://doi.org/10.1063/1.2183350

Sahu D, Panda NR and Acharya BS (2017), Effect of Gd doping on structure and photoluminescence properties of ZnO nanocrystals, Mater. Res. Express. **4:** 114001. https://doi.org/10.1088/2053-1591/aa9597

Sambasivam S, Joseph DP, Naidu SA, Hui KN, Hui KS and Choi BC (2015), Intense violet–blue emission and paramagnetism of nanocrystalline Gd^{3+} doped ZnO ceramics*, J. Adv. Ceram.* **4:** 300-306. DOI: 10.1007/s40145-015-0164-y

Shimogaki T, Kawahara H, Nakao S, Higashihata M, Ikenoue H, Nakata Y, Nakamura D and Okada T (2015), Controlling ZnOnano wire surface density during its growth by altering morphological properties of a ZnO buffer layer by UV laser irradiation, *Appl. Phys. A.* **118:** 1239-1246. http://dx.doi.org/ 10.1007/ s00339-014-8822-4

Singh AK, Viswanath V and Janu VC (2009), Synthesis, effect of capping agents, structural, optical and photoluminescence properties of ZnO nanoparticles, *J. Lumin.* **129:** 874-878. https://doi.org/ 10.1016/j.jlumin.2009.03.027

Studenikin SA, Golego N and Cocivera M (1998), Fabrication of green and photoluminescent, undoped ZnO films using spray pyrolysis, *J. Appl. Phys.* **84:** 2287-2294. https://doi.org/10.1063/1.368295

Sukumaran A, Sivanantham N, Vinoth E and Gopalakrishnan N (2021), Ferromagnetism in Gd-doped ZnO thin films mediated by defects, *Bull. Mater. Sci.* **44:** 259. http://dx.doi.org/ 10.1007/s12034-021-02550-y

Tan Y, Fang Z, Chen W and He P (2011),Structural, optical and magnetic properties of Eu-doped ZnO films,*J. Alloys Compd.* **509:** 6321-6324. https://doi.org/10.1016/j.jallcom.2011.03.084

Tawil SNM, Krishnamurthy D, Kakimi R, Emura S, Hasegawa S and Ashi H (2011), Studies on the InGaGdN/GaN magnetic semiconductor heterostructures grown by plasma-assisted molecular-beam epitaxy, *Journal of Crystal Growth.* **323:** 351-354. https://doi.org/10.1016/j.jcrysgro.2010.11.166

Thangeeswari T, Murugasen P and Velmurugan J (2015), Influence of Co and Dy doping on the optical and magnetic properties of ZnO nanoparticles for DMS application, *J. Supercond. Nov. Magn.* **28:** 2505-2515. https://doi.org/10.1007/S10948-015-3045-2

Wakano T, Fujimura N, Morinaga Y, Abe N, Ashida A and Ito T (2001), Magnetic and Magneto-Transport Properties of ZnO: Ni Films, *Physica E: Low-Dimensional Systems and Nanostructures.* **10:** 260-264. doi:10.1016/S1386-9477(01)00095-9

Wang XJ, Wang W and Liu YL (2012), Enhanced acetone sensing performance of Au nanoparticles functionalized flower-like ZnO, *Sensors Actuators B: Chemical.* **168:** 39-45. https://doi.org/10.1016/j.snb.2012.01.006

Yi XY, Ma CY, Yuan F, Wang N, Qin FW, Hu BC and Zhang QY (2017), Structural, morphological, photoluminescence and photocatalytic properties of Gd doped ZnO films, *Thin Solid Films.* **636:** 339-345. https://-doi.org/10.1016/j.tsf.2017.05.020